ISSN 1749-3889 (print), 1749-3897 (online)
International Journal of Nonlinear Science
Vol.27(2019) No.1,pp.43-52

Numerical Studies on Nanofluid Flow over a Porous Vertical Plate with Internal Heat Generation and Thermal Radiation

Hiranmoy Mondal [1] *, Poulomi De[2], Sicelo P. Goqo[1], Precious Sibanda[1]
[1] School of Mathematics, Statistics and Computer Science, University of KwaZulu-Natal, Private Bag X01, Scottsvile, Pietermaritzburg-3209, South Africa
[2] Department of Mathematics, School of Advanced Sciences, VIT University, Chennai Campus, Chennai-600127, Tamil Nadu, India
(Received 22 May 2018, accepted 24 December 2018)

Abstract: This paper deals a numerical investigation on mixed convection flow with nanofluid through a porous medium due to the combined effects of thermal radiation and internal heat generation. The energy equation accounts for heat generation or absorption and the diffusing species is included in the mass diffusion equation. The model used for the nanofluid incorporates the effects of Brownian motion and thermophoresis. The nonlinear equations of the momentum, energy, and concentration are obtained into a dimensionless form by introducing a suitable group of similarity transformations. The transformed coupled non-linear ordinary differential equations are solved numerically using appropriate boundary conditions for the various values of physical parameters. The effects of various physical parameters on the dimensionless velocity, temperature, and concentration profiles are investigated through graphs.

Keywords: Mixed convection; Nanofluids; Porous medium; Hheat generation; Thermal radiation

1 Introduction

Improving the technology, limit in enhancing the performance of conventional heat transfer is a main issue owing to low thermal conductivity of the most common fluids such as water, oil, and ethylene-glycol mixture. Since the thermal conductivity of solids is often higher than that of liquids, the idea of adding particles to a conventional fluid to enhance its heat transfer characteristics emerged. Among all dimensions of particles such as macro, micro, and nano, due to some obstacles in the pressure drop through the system or keeping the mixture homogenous, nanoscaled particles have attracted more attention. These tiny particles are fairly close in size to the molecules of the base fluid and thus can realize extremely stable suspensions with slight gravitational settling over long periods of time. Choi [1] point out the engineered colliods composed of nanoparticles dispersed in a base fluid. The thermal conductivity of ordinary heat transfer fluids is not adequate to meet today's cooling rate requirements. Nanofluids have been shown to increase the thermal conductivity and convective heat transfer performance of base fluids. Nanofluids attract a great deal of interest with their enormous potential to provide enhanced performance properties particularly with respect to heat transfer. Nanofluids are used for cooling of microchips in computers and other electronics which use microfluidic applications. Eastman et al. [2] have investigated the enhanced thermal conductivity through the development of nanofluids. Mondal et al. [3] have reviewed the convective heat transfer enhancement with nanofluids. Daungthongsuk and Wongwises [4] have studied the critical review of convective heat transfer of nanofluids. Pal and Mondal [5] have studied the effects of heat and mass transfer over a Stretching Sheet with thermal radiation. Recently, Sithole et al. [6,7] investigated the magnetohydrodynamic nanofluid flow over a convectively heated stretching sheet with nonlinear thermal radiation and chemical reaction.

For years, many researchers have paid much attention to viscous fluid motion near the stagnation region of a solid body, where "body" corresponds to either fixed or moving surfaces in a fluid. This multidisciplinary flow has frequent applications in high speed flows, thrust bearings, and thermal oil recovery. Besides stagnation point flow, stretching

*Corresponding author. *E-mail address*: hiranmoymondal@yahoo.co.in

IJNS.2019.02.15/1032

surfaces have a wide range of applications in engineering and several technical purposes particularly in metallurgy and polymer industry, for instance, gradual cooling of continuous stretched metal or plastic strips which have multiple applications in mass production. Magyari and Keller [8] have studied the heat and mass transfer in the boundary layers on an exponentially stretching continuous surface. Al-Odat et al. [9] have investigated the thermal boundary layer on an exponentially stretching continuous surface in the presence of magnetic field effect. Khan and Sanjayanand [10] have studied viscoelastic boundary layer flow and heat transfer over an exponential stretching sheet. Afzal [11] has studied momentum and thermal boundary layers over a two-dimensional or axisymmetric non-linear stretching surface in a stationary fluid. Kumari and Nath [12] have studied steady mixed convection flow of Maxwell fluid over an exponentially stretching vertical surface with magnetic field and viscous dissipation. Lok and Pop [13] have investigated stretching or shrinking sheet problem for unsteady separated stagnation point flow. Mahapatra and Nandy [14] have studied slip effects on unsteady stagnation point flow and heat transfer over a shrinking sheet.

At high operating temperatures especially in the field of space technology, radiation effect is quite significant. Many processes in engineering areas occur at high temperatures and the knowledge of radiation heat transfer becomes very important, particularly in designing pertinent equipment. Mahapatra et al. [15] have investigated oblique stagnation point flow and heat transfer towards a shrinking sheet with thermal radiation. Singh [16] has analyzed heat source and radiation effects on magnetoconvection flow of a viscoelastic fluid past a stretching sheet with Kummer's functions. Patil et al. [17] have investigated effects of chemical reaction on mixed convection flow of a polar fluid through a porous medium in presence of internal heat generation. Poornima and Reddy [18] have studied the radiation effects on MHD free convective boundary layer flow of nanofluids over a non linear stretching sheet. Pal and Mondal [19] have investigated the hydromagnetic non-Darcy flow and heat transfer over a stretching sheet in the presence of thermal radiation and ohmic dissipation. Mostafa [20] has studied thermal radiation effect on unsteady MHD free convection flow past a vertical plate with temperature dependent viscosity.

In the present paper, the authors propose to study the effects of heat and mass transfer of a nanofluids through porous medium with thermal radiation and internal heat generation. The transformed dimensionless governing equations are solved numerically. The effects of various physical parameters on velocity, temperature, concentration fields as well as on skin-friction coefficient. Nusselt number and Sherwood number are analyzed.

2 Formulation of the problem

We consider the two-dimensional mixed convection flow of a viscous incompressible nanofluid through a porous medium over a semi-infinite vertical porous plate. The x-axis is taken along the vertical plate and y-axis is normal to it. The surface is maintained at a prescribed heat flux q_w as well as a mass flux m_w. A heat source or sink is placed within the flow to allow possible heat generation or absorption effects. The concentration of diffusing species is assumed to be very small in comparison with other chemical species far from the surface C_∞, and is infinitely small. Hence the Soret and Dufour effects are neglected. All thermo-physical properties of the fluid in the flow model are assumed to be constant except the density variations causing the body force term in the momentum equation. The Boussinesq approximation is invoked for the fluid properties to relate density changes, and to couple in this way the temperature and concentration fields, $g[\beta_T(T-T_\infty)+\beta_c(C-C_\infty)]$ to the flow field. Under the above assumptions, the equations of conservation of mass, momentum, energy, and concentration governing the problem of mixed convection boundary layer flow along a plate in a porous medium (see Patil et al. [17]) are given by:

(i) Conservation of mass:

$$\frac{\partial u}{\partial x}+\frac{\partial v}{\partial y}=0. \tag{1}$$

(ii) Conservation of momentum:

$$u\frac{\partial u}{\partial x}+v\frac{\partial u}{\partial y}=(\nu+\nu_r)\frac{\partial^2 u}{\partial y^2}+g[\beta_T(T-T_\infty)+\beta_c(C-C_\infty)]-\frac{\nu+\nu_r}{K}(u-U_\infty). \tag{2}$$

(iii) Energy equation:

$$u\frac{\partial T}{\partial x}+v\frac{\partial T}{\partial y}=\frac{k}{\rho C_p}\frac{\partial^2 T}{\partial y^2}+\frac{Q_0}{\rho C_p}(T-T_\infty)+\tau\left[D_B\frac{\partial C}{\partial y}\frac{\partial T}{\partial y}+\frac{D_T}{T_\infty}\left(\frac{\partial T}{\partial y}\right)^2\right]-\frac{1}{\rho C_p}\frac{\partial q_r}{\partial y}. \tag{3}$$

(iv) Mass Diffusion of species equation:

$$u\frac{\partial C}{\partial x}+v\frac{\partial C}{\partial y}=D_B\frac{\partial^2 C}{\partial y^2}+\frac{D_T}{T_\infty}\frac{\partial^2 T}{\partial y^2}. \tag{4}$$

The appropriate boundary conditions are:

$$\begin{aligned} y=0: \quad u=0, \quad v=0, \quad -k\frac{\partial T}{\partial y}=q_w, \quad -D\frac{\partial C}{\partial y}=m_w,\\ y\to\infty: \quad u\to U_\infty(x), \quad T\to T_\infty, \quad C\to C_\infty, \end{aligned} \tag{5}$$

where u and v denote the velocity components in x- and y-direction, respectively. ν is kinematic viscosity, ν_r is rotational kinematic viscosity, g is acceleration due to gravity, β_T and β_C are the volumetric coefficients of the thermal and concentration expansions, respectively, T is temperature in the boundary layer, T_∞ is temperature of fluid far away from the wall, C is species concentration, C_∞ is species concentration far away from the wall, K is permeability of the porous medium, ρ is the density of the fluid, C_p is the specific heat at constant pressure, Q_0 is the heat generation coefficient, D is the mass diffusivity, q_w is the heat flux per unit area at the plate, m_w is the mass flux per unit area at the plate and k is the thermal conductivity of the fluid.

In order to obtain similarity solution of the problem we introduce the following non-dimensional variables:

$$\begin{aligned} &\xi=\frac{x}{L}, \quad \eta=\left(\frac{U_\infty}{\nu x}\right)^{1/2}y, \quad \psi(x,y)=(\nu U_\infty x)^{1/2}f(\xi,\eta), \quad (T-T_\infty)=\left(\frac{q_w}{k}\right)\left(\frac{\nu x}{U_\infty}\right)^{1/2}\theta(\xi,\eta),\\ &(C-C_\infty)=\left(\frac{m_w}{D}\right)\left(\frac{\nu x}{U_\infty}\right)^{1/2}\phi(\xi,\eta), \quad u=U_\infty\frac{\partial f}{\partial\eta}, \quad v=-\frac{(\nu U_\infty x)^{1/2}}{2x}(f(\xi,\eta)+2\xi f_\xi-\eta f_\eta),\\ &f_\eta(\xi,\eta)=F(\xi,\eta), \end{aligned} \tag{6}$$

where L is the characteristics length and ξ and η are the transformed variables, respectively.

Defining the stream function in the usual way such that $u=\frac{\partial\psi}{\partial y}$ and $v=-\frac{\partial\psi}{\partial x}$ and substituting Eq. (6) in Eqs. (2), (3), and (4), we obtain the following transformed equations:

$$f^{'''}+\frac{f}{2(1+\alpha)}f^{''}-\frac{\xi}{DaRe_L}(f^{'}-1)+\frac{\lambda}{(1+\alpha)}\xi^{3/2}(\theta+N\phi)=\frac{\xi}{1+\alpha}[f^{'}\frac{\partial f^{'}}{\partial\xi}-\frac{\partial f}{\partial\xi}f^{''}], \tag{7}$$

$$(1+Nr)\theta^{''}+\frac{Pr}{2}f\theta^{'}+Pr\left(Q\xi-\frac{1}{2}f^{'}\right)\theta+Pr(Nb\theta^{'}\phi^{'}+Nt\theta^{'2})=Pr\xi[f^{'}\frac{\partial\theta}{\partial\xi}-\frac{\partial f}{\partial\xi}\theta^{'}], \tag{8}$$

$$\phi^{''}+\frac{Le}{2}f\phi^{'}-\frac{Le}{2}f^{'}\phi+\frac{Nt}{Nb}\theta^{''}=Le\xi[f^{'}\frac{\partial\phi}{\partial\xi}-\frac{\partial f}{\partial\xi}\phi^{'}], \tag{9}$$

where

$$\begin{aligned} &\alpha=\frac{\nu_r}{\nu}, \quad Re_L=\frac{U_\infty L}{\nu}, \quad Da=\frac{K}{L^2}, \quad Q=\frac{Q_0L}{\rho C_pU_\infty}, \quad Gr=\frac{g\beta_Tq_wL^4}{k\nu^2Re_L^{1/2}}, \quad Gr^*=\frac{g\beta_Cm_wL^4}{D\nu^2Re_L^{1/2}},\\ &\lambda=\frac{Gr}{Re_L^2}, \quad \lambda^*=\frac{Gr^*}{Re_L^2}, \quad N=\frac{\lambda^*}{\lambda}, \quad Pr=\frac{\rho\nu C_p}{k}, \quad Nr=\frac{16\sigma^*T_\infty^3}{3K^*k},\\ &Le=\frac{\nu}{D_B}, \quad Nb=\frac{(\rho c)_pD_B(C_w-C_\infty)}{(\rho c)_f\nu}, \quad Nt=\frac{(\rho c)_pD_T(T_w-T_\infty)}{(\rho c)_f\nu T_\infty} \end{aligned} \tag{10}$$

are the material parameter characterizing the polarity of the fluid, Reynolds number, Darcy number, dimensionless heat generation or absorption parameter, Grashof number due to temperature, Grashof number due to concentration, Buoyancy parameter due to temperature, Buoyancy parameter due to concentration gradient, ratio of buoyancy forces, Prandtl number, Thermal radiation parameter, Lewis number, Brownian motion parameter, and Thermophoresis parameter, respectively.

The dimensionless boundary conditions are

$$\eta = 0: \quad F = f^{'} = 0, \quad \theta^{'} = -1, \quad \phi^{'} = -1,$$
$$\eta \to \infty: \quad f^{'} = F \to 1, \quad \theta \to 0, \quad \phi \to 0. \tag{11}$$

It is worth mentioning here that $T_w > T_\infty$ refers to a heated plate (assisting flow) and $T_w < T_\infty$ for a cooled plate (opposing flow). Therefore, the mixed convection (buoyancy) parameter appearing in (7) $\lambda > 0$ indicates for assisting flow and $\lambda < 0$ for opposing flow, respectively.

The momentum Eq.(7) is coupled with all the other equations of the system. The material parameter α appearing in (7) is the non-dimensional parameter which characterize the polarity of the fluid represents the ratio between the rotational kinematic viscosity (ν_r) and kinematic viscosity (ν). When $\alpha = 0$, the problem reduces to Newtonian case. The ratio of buoyancy forces N appearing in (7) is zero for no buoyancy effect due to mass diffusion, is infinite for no buoyancy effect due to thermal diffusion, is unity for thermal and mass buoyancy forces of the same strength, positive (> 0) for the combined buoyancy forces driving the flow and negative (< 0) for the buoyancy forces opposing each other. The heat generation or absorption parameter Q appearing in (8) is the non-dimensional parameter based on the amount of heat generated or absorbed per unit volume given by $Q_0(T - T_\infty)$, Q_0 being constant coefficient, which may take either positive or negative values. The source term represents the heat generation when Q is positive (> 0) the heat absorption when Q is negative (< 0). The parameter Q is zero in case of no heat source.

Important physical parameters for the flow, heat and mass transfer characteristics are the local skin-friction coefficient, local Nusselt number and the local Sherwood number which can be obtained from velocity, temperature, and concentration fields $f^{'}(\xi, \eta)$, $\theta(\xi, \eta)$ and $\phi(\xi, \eta)$ their derivatives from the following relations:

$$Re_L^{1/2} C_{fx} = 2(1 + \alpha)\xi^{-1/2} f^{"}(\xi, 0), \tag{12}$$

$$Re_L^{-1/2} Nu_x = \frac{\xi^{1/2}}{\theta(\xi, 0)}, \tag{13}$$

$$Re_L^{-1/2} Sh_x = \frac{\xi^{1/2}}{\phi(\xi, 0)}. \tag{14}$$

3 Results and discussions

Numerical solutions to study the various governing parameter effects on mixed convection flow of a nanofluid over a stretching sheet in the presence of internal heat generation and thermal radiation through a porous medium are reported. The results are presented graphically in Figs. 1-23 and conclusions are drawn to analyze the effects of various physical quantities of interest on the velocity, temperature, and concentration distribution that have significant effects. Comparisons of the present results with previously published works (see Table 1) are performed and excellent agreement have been obtained.

Figs. 1-3 display the velocity, temperature, and concentration distribution for different values of the buoyancy ratio parameter N. It is observed from Fig. 1 that, for buoyancy-induced aiding flow $N > 0$, the buoyancy forces show significant overshoot in the velocity profiles near the wall. As N increases, the velocity increases for buoyancy assisting flow $(\lambda > 0)$ near the wall. The physical reason is that the buoyancy forces act like a pressure gradient which accelerates/ decelerates the fluid within the boundary layer. The effect of N on the velocity profile is significant because the parameter N is explicitly present only in the momentum equation. In fact, the combined effects of an assisting buoyancy force due to thermal and concentration gradients and heat generation act like a favorable pressure gradient which enhances the fluid acceleration. Further, it is observed from Fig. 2 that increasing the value of N has the tendency to decrease the fluid wall temperature. Fig. 3 shows that an increase in N causes an distinct fall in the concentration profile. All profiles decay to the free stream value of zero as $\eta \to \infty$. As N increases, the ratio of concentration Grashof number is higher than the thermal Grashof number. Therefore, we conclude from the results that the problem is predominantly governed by thermal buoyancy forces.

The resulting profiles of dimensionless velocity, temperature, and concentration for various values of the heat generation or absorption parameter Q are illustrated in Figs. 4-6. It is noted that owing to the presence of a heat generation or a heat source effect, the thermal state of the fluid increases. Hence, the temperature of the fluid increases within the boundary layer. In the event that the strength of the heat source is relatively large, an overshoot is observed in the temperature profiles within the thermal boundary layer as can be seen from Fig. 5. Fig. 4 displays that, the velocity profile has

increase with a thin velocity boundary layer whereas decrease for concentration boundary layer which can be seen from Fig. 6.

The effect of Brownian motion parameter Nb on velocity $f'(\xi,\eta)$, temperature $\theta(\xi,\eta)$, and concentration $\phi(\xi,\eta)$ are shown in Figs. 7-9. The boundary layer profiles for the temperature are of the same form as in the case of regular heat transfer fluids. The fluid velocity and temperature in the boundary layer increases with the increase in the Brownian motion parameter Nb. But, the nanoparticle volume fraction profile decreases with the increase in the Brownian motion parameter Nb. Brownian motion serves to warm the boundary layer and simultaneously exacerbates particle deposition away from the fluid regime (onto the surface), thereby accounting for the reduced concentration magnitudes in Fig. 9. The Brownian motion of nanoparticles can enhance thermal conduction via one of two mechanisms, either a direct effect owing to nanoparticles that transport heat or alternatively via an indirect contribution due to micro-convection of fluid surrounding individual nanoparticles. For small particles, Brownian motion is strong and the parameter Nb will have high values, the converse is the case for large particles and clearly Brownian motion does exert a significant enhancing influence on both temperature and concentration profiles.

Figs. 10-12 illustrate profiles for velocity $f'(\xi,\eta)$, temperature $\theta(\xi,\eta)$, and concentration $\phi(\xi,\eta)$ distributions for various values of the thermophoretic parameter Nt. It is noted that both fluid velocity and temperature increases whereas the nanoparticle volume fraction decreases with increase in Nt. It is observed that an increase in Nt, results in an increase of the temperature and concentration differences between the stretching surface and the ambient fluid. Thus, it is noticed that the velocity and temperature profiles increase but the thickness of the concentration boundary layer decrease with the increase of the values of thermophoretic parameter Nt. We notice that, positive Nt indicates a cold surface while negative to a hot surface. For hot surfaces, thermophoresis tends to blow the nanoparticle volume fraction boundary layer away from the surface since a hot surface repels the sub-micron sized particles from it, thereby forming a relatively particle-free layer near the surface. As a consequence, the nanoparticle distribution is formed just outside. In particular, the effect of increasing the thermophoretic parameter Nt is limited to increasing slightly the wall slope of the nanoparticle volume fraction profiles but decreasing the nanoparticle volume fraction.

Figs. 13-15 illustrate the influence of the buoyancy parameter λ on the temperature $\theta(\xi,\eta)$ and concentration $\phi(\xi,\eta)$ profiles, respectively. An increase in the buoyancy parameter λ induces a strong reduction in the fluid temperature and hence, results into a thinner thermal boundary layer. It is noted from Fig. 15 that an increase in the value of λ leads to a fall in the concentration profile.

The effect of Prandtl number Pr on velocity and concentration profiles are depicted graphically in Fig. 16 and Fig. 18. With an increase in the values of Prandtl number results in increasing velocity profile whereas concentration boundary layer decrease. The effect of Prandtl number Pr on the heat transfer process is shown by the Fig. 17. This figure reveals that an increase in Prandtl number Pr increases far away from the surface whereas decreases at the surface, because, thermal boundary layer thickness decreases with an increase in Prandtl number Pr. In short, an increase in the Prandtl number means the slow rate of thermal diffusion. The effects of Prandtl on a nanofluid is similar to what has already been observed in common fluids qualitatively but they are different quantitatively. Therefore, this properties are inherited by nanofluids.

Fig. 20 displays the effect of Lewis number Le on the concentration profile. As the Lewis number increases concentration decreases. The decrease in concentration profiles are accompanied by simultaneous reductions in concentration boundary layers thicken and this is the analogous to the effect of increasing the Prandtl number on the thickness of a thermal boundary layer. It is evident from the Fig. 20 that the concentration C takes its limiting value C_∞, for higher values of the dimensionless distance η. From this figure, we observe that when the concentration difference ΔC is maintained constant, the dimensionless concentration profile decreases, since that the values of Lewis number Le increases.

The variations of the skin-friction coefficient, Nusselt number, Sherwood number and wall stress coefficient as a function of Nb for various values of Nt are shown in Figs. 21- 23. It can be observed from Figs. 21-22 that the effect of increasing Nb increases the skin-friction coefficient and Nusselt number for all the values of Nt but the reverse effect can be seen from Fig. 23 for the Sherwood number.

Table 1: Comparison of $Nu_x Re_L^{-1/2}$ for selected values of Pr to previously published work with $\Delta = 0.0$, $\xi = 1.0$, $\lambda = 0.0$, $Nb = 0.1$, $Nt = 0.0$, $Le = 0.0$.

Pr	Lee et al. [21]	Chang and Lee [22]	Patil [23]	Present Results
0.1	0.2634	0.2634	0.263914	0.26388
0.7	0.4838	0.4838	0.483776	0.48394
7.0	0.8697	0.8697	0.870026	0.86890

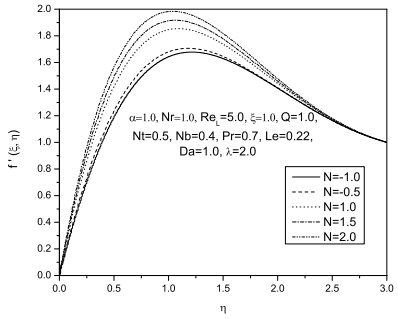

Figure 1: Velocity profile vs. η for different values of N.

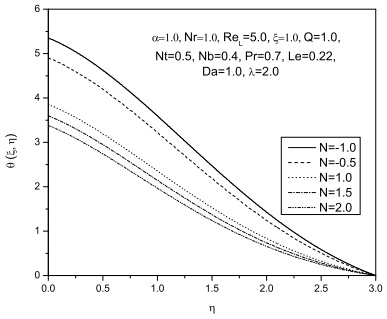

Figure 2: Temperature profile vs. η for different values of N .

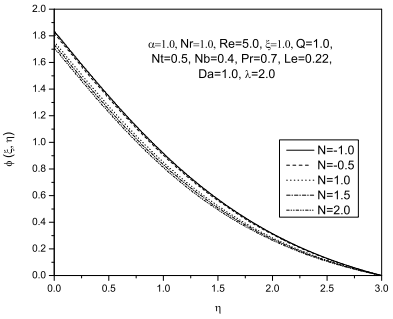

Figure 3: Concentration profile vs. η for different values of N .

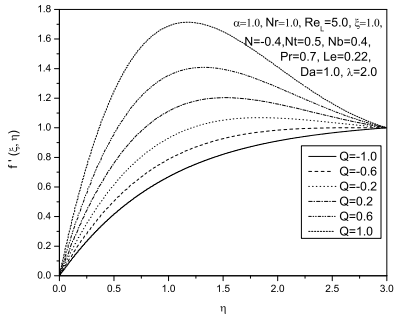

Figure 4: Velocity profile vs. η for different values of Q .

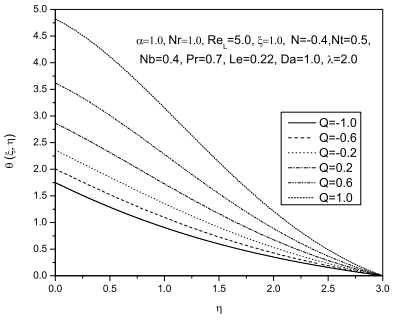

Figure 5: Temperature profile vs. η for different values of Q .

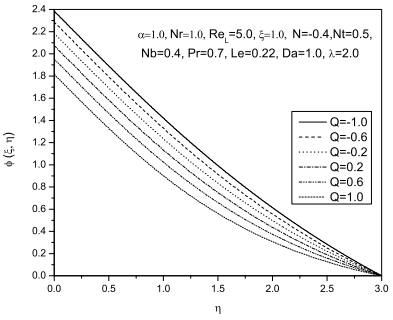

Figure 6: Concentration profile vs. η for different values of Q .

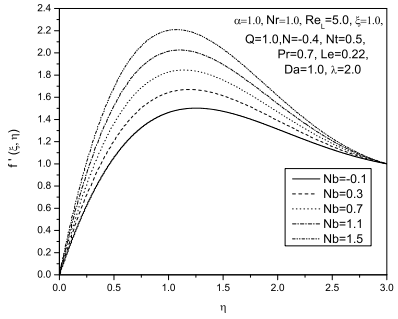

Figure 7: Velocity profile vs. η for different values of Nb .

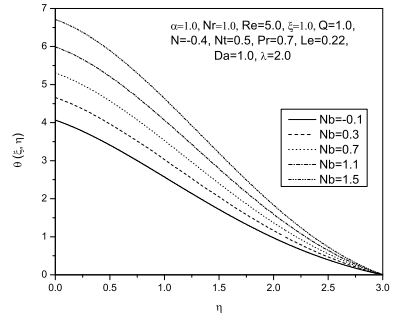

Figure 8: Temperature profile vs. η for different values of Nb .

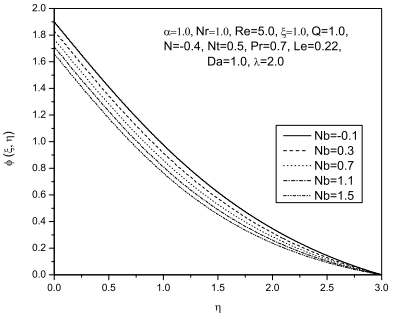

Figure 9: Concentration profile vs. η for different values of Nb .

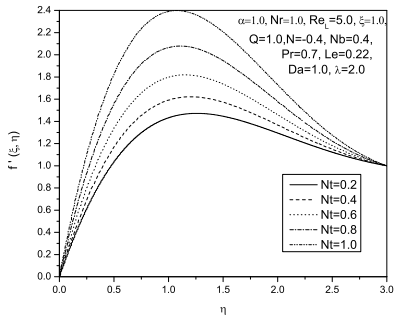

Figure 10: Velocity profile vs. η for different values of Nt .

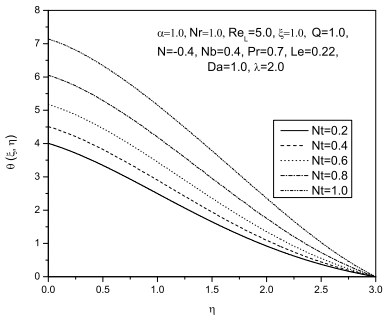

Figure 11: Temperature profile vs. η for different values of Nt .

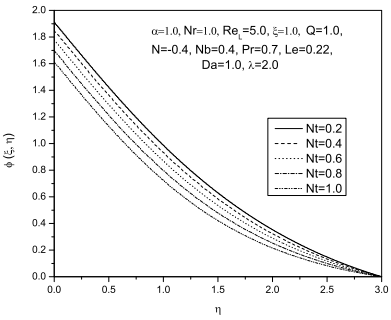

Figure 12: Concentration profile vs. η for different values of Nt .

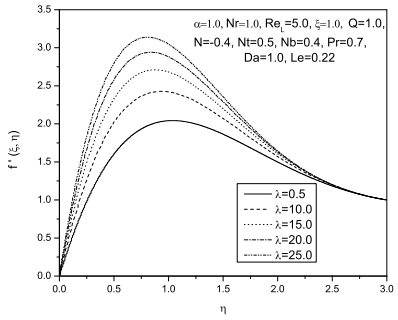

Figure 13: Velocity profile vs. η for different values of λ .

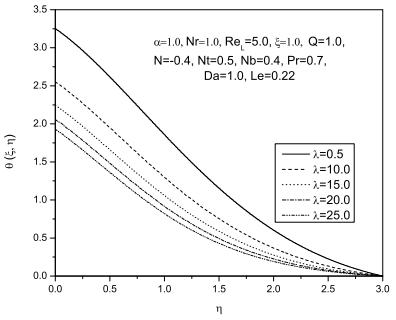

Figure 14: Temperature profile vs. η for different values of λ .

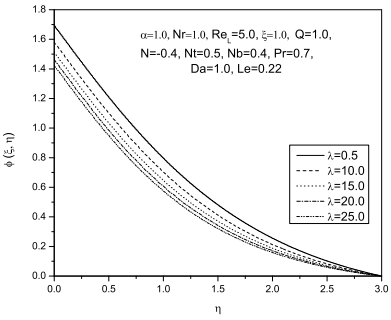

Figure 15: Concentration profile vs. η for different values of λ .

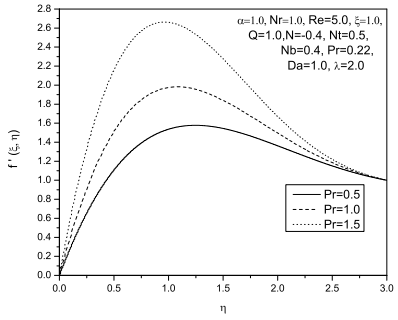

Figure 16: Velocity profile vs. η for different values of Pr .

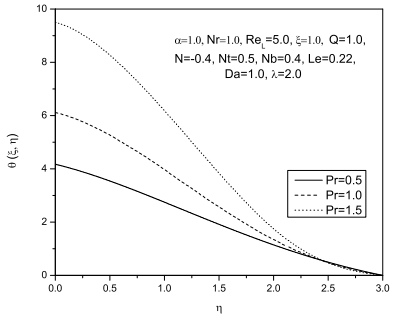

Figure 17: Temperature profile vs. η for different values of Pr .

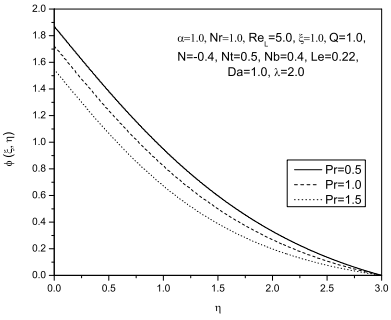

Figure 18: Concentration profile vs. η for different values of Pr .

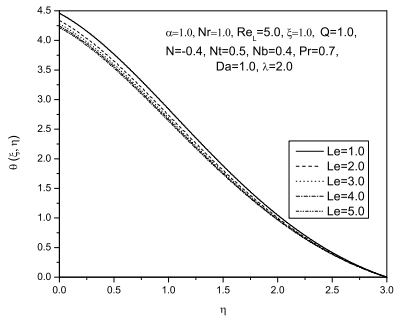

Figure 19: Temperature profile vs. η for different values of Sc .

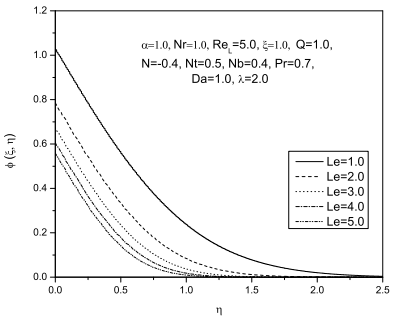

Figure 20: Concentration profile vs. η for different values of Sc .

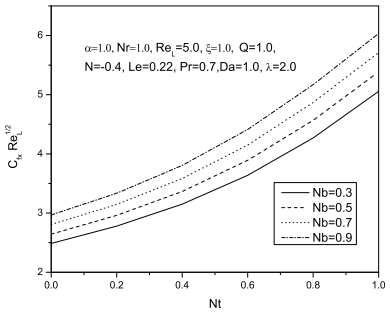

Figure 21: Variation in skin-friction coefficient with Nb for various values of Nt.

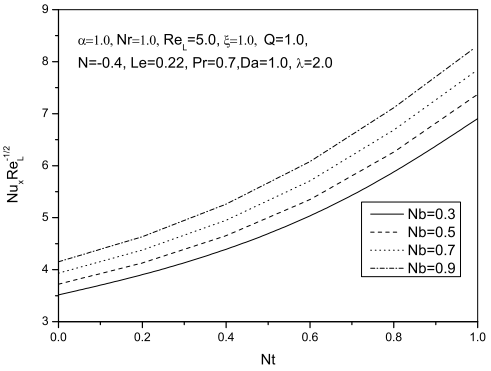

Figure 22: Variation in Nusselt number with Nb for various values of Nt.

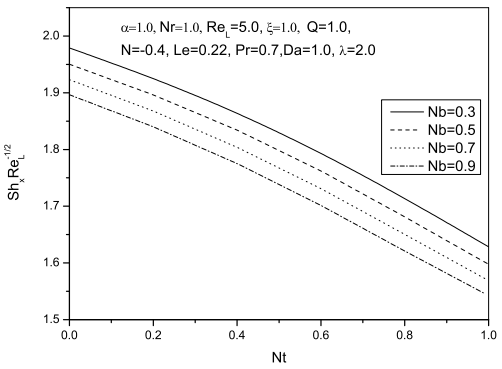

Figure 23: Variation in Sherwood number with Nb for various values of Nt.

4 Conclusion

A detailed numerical study has been carried out for mixed convection flow of a nanofluid through a porous medium in the presence of internal heat generation or absorption and thermal radiation. A transformed set of non-similar equations was obtained and were solved numerically. The effects of various physical parameter were examined in boundary layer and analyzed in details. Following conclusions are drawn from the numerical results:

1. The effect of Prandtl number Pr and the buoyancy ratio parameter N are found to increase velocity profile whereas produces a significant decrease in the thermal and concentration boundary layer.

2. The heat generation or absorption parameter Q, Brownian motion parameter Nb, and thermophoresis parameter Nt increases the thickness of the velocity and thermal boundary layers while the concentration boundary layer thickness reduces.

3. The effect of Lewis number Le and the buoyancy parameter λ decreases the thermal and concentration boundary layer.

4. The effect of thermal radiation parameter Nr is found to increase in velocity and thermal boundary layer.

5. The effects of Brownian motion parameter Nb and thermophoresis parameter Nt are found to be significant on the skin-friction coefficient and Nusselt number whereas reverse effect occur for Sherwood number.

Acknowledgments

This work was supported by the Claude Leon Foundation Postdoctoral Fellowship, University of KwaZulu-Natal, and the National Research Foundation of South Africa (Grant Number: 107202).

Conflict of interest

In this paper there is no conflict of interest.

References

[1] S.U.S. Choi. Enhancing thermal conductivity of fluids with nanoparticles. *ASME Fluids Eng. Div.*, 231(1995): 99-105.

[2] J.A. Eastman, U.S. Choi, S. Li, L.J. Thompson and S. Lee. Enhanced Thermal Conductivity Through the Development of Nanofluids, Proceedings of Symposium on Nanophase and Nanocomposite Materials. *Materials Research Society*, 457(1997): 3-11.

[3] H. Mondal, P. De, S. Chatterjee, P. Sibanda and P.K. Roy. MHD Three-Dimensional Nanofluid Flow on a Vertical Stretching Surface with Heat Generation/Absorption and Thermal Radiation. J*ournal of Nanofluids,* 6(2017): 189-195.

[4] W. Daungthongsuk and S. Wongwises. A critical review of convective heat transfer of nanofluids. *Renewable and Sustainable Energy Reviews*, 11(5)(2007): 797-817.

[5] D. Pal and H. Mondal. Non-Darcian Buoyancy Driven Heat and Mass Transfer over a Stretching Sheet in a Porous Medium with Radiation and Ohmic Heating. *Int. Journal of Nonlinear Sciences,* 14(1)(2012): 115-123.

[6] H. Sithole, H. Mondal and P. Sibanda. Entropy generation in a second grade magnetohydrodynamic nanofluid flow over a convectively heated stretching sheet with nonlinear thermal radiation and viscous dissipation. *Results in Physics,* 9(2018): 1077-1085.

[7] H. Sithole, H. Mondal, S. Goqo, P. Sibanda and S. Motsa. Numerical simulation of couple stress nanofluid flow in magneto-porous medium with thermal radiation and a chemical reaction. *Applied Mathematics and Computation*, 339(2018): 820-836.

[8] E. Magyari and B. Keller. Heat and mass transfer in the boundary layers on an exponentially stretching continuous surface. *J. Phys. d. Appl. Phys.*, 32(2014): 577-585.

[9] M.Q. Al-Odat, R.A. Damseh and T.A. Al-Azab. Thermal boundary layer on an exponentially stretching continuous surface in the presence of magnetic field effect. *Int J Appl Mech Eng*, 11(2006): 289-299.

[10] S.K. Khan and E. Sanjayanand. Viscoelastic boundary layer flow and heat transfer over an exponential stretching sheet. *Int. J. Heat Mass Transf.*, 48(8)(2005): 1534-1542.

[11] N. Afzal. Momentum and thermal boundary layers over a two-dimensional or axisymmetric non-linear stretching surface in a stationary fluid. *Int. J. Heat Mass Transf.*, 53(1-3)(2010): 540-547.

[12] M. Kumari and G. Nath. Steady mixed convection flow of Maxwell fluid over an exponentially stretching vertical surface with magnetic field and viscous dissipation. *Meccanica*, 49(2014): 1263-1274.

[13] Y.Y. Lok and I. Pop. Stretching or shrinking sheet problem for unsteady separated stagnation point flow. *Meccanica*, 49(2014): 1479-1492.

[14] T.R. Mahapatra and S.K. Nandy. Slip effects on unsteady stagnation point flow and heat transfer over a shrinking sheet. *Meccanica*, 48(2013): 1599-1606.

[15] T.R. Mahapatra, S.K. Nandy and A.S. Gupta. Oblique stagnation point flow and heat transfer towards a shrinking sheet with thermal radiation. *Meccanica*, 47(2012): 1325-1335.

[16] A.K. Singh. Heat source and radiation effects on magnetoconvection flow of a viscoelastic fluid past a stretching sheet: analysis with Kummer's functions. *Int Commun Heat and Mass Transfer*, 35(5)(2008): 637-642.

[17] P.M. Patil, A.J. Chamkha and S. Roy. Effects of chemical reaction on mixed convection flow of a polar fluid through a porous medium in presence of internal heat generation. *Meccanica*, 47(2012): 483-499.

[18] T. Poornima and N.B. Reddy. Radiation effects on MHD free convective boundary layer flow of nanofluids over a non linear stretching sheet. *Advances in Applied Science Research,* 4(2)(2013): 190-202.

[19] D. Pal and H. Mondal. Hydromagnetic non-Darcy flow and heat transfer over a stretching sheet in the presence of thermal radiation and Ohmic dissipation. *Commun Nonlinear Sci. Numer. Simulat.*, 15(2010): 1197-1209.

[20] A.A. Mostafa. Thermal radiation effect on Unsteady MHD free convection flow past a vertical plate with temperature dependent viscosity. *The Canadian Journal of Chemical Engineering*, 87(1)(2009): 171 - 181.

[21] S.L. Lee, T.S. Chen and B.F. Armaly. Mixed convection along vertical cylinders and needles with uniform surface heat flux. *ASME J. Heat Transfer*, 109(1987): 711-716.

[22] C.L. Chang and Z.Y. Lee. Free convection on a vertical plate with uniform and constant heat flux in a thermally stratified micropolar fluid. *Mechanics Research Communications*, 35(2008): 421-427.

[23] P.M. Patil. Chemical Reaction Effects on Free Convective Flow of a Polar Fluid from a Vertical Plate with Uniform Heat and Mass Fluxes. *IOSR Journal of Mathematics*, 6(5) (2013): 66-85.